Ab Initio Study of Coupled Electron Transfer/Proton Transfer in Cytochrome *c* Oxidase

Dana B. Moore and Todd J. Martínez*

Department of Chemistry and The Beckman Institute, University of Illinois, Urbana, Illinois 61801

Received: July 23, 1999; In Final Form: October 8, 1999

The coupled electron/proton transfer mechanism of cytochrome *c* oxidase is investigated using ab initio electronic structure theory. We predict the location and identity of the Fe and Cu ligands in the oxidized (O), partially reduced (E), and fully reduced (R) forms of the enzyme. Our calculations suggest that a tyrosine residue in close proximity to the active site is deprotonated during the enzymatic cycle. These predictions are consistent with experimental evidence and provide a molecular explanation for both the observed antiferromagnetic coupling of Fe^{3+} and Cu^{2+} and the distinction between "fast" and "slow" forms of the oxidized enzyme.

Introduction

Charge transfer processes, both of electron transfer (ET) and proton transfer (PT) varieties, play a prominent role in chemistry and biology. Thus, it is natural that the more complex *coupled* electron and proton transfer processes should also be of keen interest. Such coupled ET/PT processes are the *raison d'être* of the terminal oxidase enzymes, such as cytochrome *c* oxidase (CcO).[1−4] These transmembrane enzymes are the workhorses of respiration, converting four electrons, eight protons, and an oxygen molecule into water and electrochemical energy stored in the form of a pH gradient across the mitochondrial cell membrane. This process is catalyzed by a heterogeneous binuclear transition metal center containing heme Fe and Cu (these metal ions are denoted Fe_{a3} and Cu_B in the following). Because of its pivotal role in respiration, the elucidation of the molecular mechanism of CcO and related enzymes has been a major goal of bioenergetics for several decades. Furthermore, direct four-electron reduction of O_2 would be advantageous for fuel cells, motivating many efforts to duplicate this functionality within a smaller molecule.[5,6] Collman has recently reported success on this front with a close structural analogue of the binuclear Fe/Cu active site of CcO.[7]

A major advance in the understanding of CcO was recently made through the successful crystallization and X-ray structural analysis of both mammalian[8] and bacterial[9,10] forms of CcO. While the first work was limited to the structure of the oxidized (O) form of the enzyme, the latest results[11] also capture the enzyme in various stages of reduction prior to O_2 binding. The binuclear transition metal ion centers of the bacterial and mammalian enzymes were observed to be nearly identical, supporting previous arguments based on spectroscopic evidence that the mechanisms of the family of CcO enzymes are highly similar and the binuclear center plays a key role. Yet, knowledge of the atomic structure of this molecular machine is only the starting point for a detailed analysis of the underlying mechanism.[12,13] For example, with present-day crystallographic techniques on such large molecules (there are more than 14 000 heavy atoms in the mammalian CcO enzyme), it is not possible to observe hydrogen atoms reliably, especially when these are in close proximity to transition metals. This makes the precise identification of ligands in the binuclear center during turnover particularly vexing. Yet the details of proton motion are crucial to understanding the mechanisms of CcO.

Ab initio quantum chemistry can provide a powerful tool to bridge the gap between experiment and the chemical mechanism for biological molecules. Goddard has played a key role in demonstrating this,[14−21] and at the same time has made great advances in our understanding of transition metal catalyzed reactions.[22−28] The present work touches on both of these areas, combining the experimental X-ray structural information with ab initio quantum chemical techniques in order to suggest the chemical intermediates involved in the early stages of the CcO enzymatic cycle. The application of ab initio quantum chemistry to metalloenzyme mechanisms involving more than one transition metal is still quite new[29−31] and the accuracy that can be expected is not well known. One should thus be cautious in interpreting the results, and critical comparisons with experiment are crucial. As we show below, the predictions of the model adopted in this work agree with known experimental facts on many counts, lending credibility to the model.

The basic catalytic mechanism of CcO is indicated schematically in Figure 1. The active site of the enzyme contains two transition metal ions, Fe_{a3} and Cu_B, separated by ≈5 Å. The Cu_B ion is ligated by three histidine residues and the Fe_{a3} is in the heme *a* form. The absence of nonproteinaceous metal ligands in the sketch is meant only to imply lack of experimental consensus and should not be taken literally. Indeed, one of the goals of this work is to determine what the correct ligands are. Electrons are transferred to the binuclear center from either a second heme moiety (heme *a*) or a binuclear copper center (Cu_A). Protons are supplied from the cytoplasm and the fate of the water molecules resulting from reduction of O_2 is not characterized.

One of the fundamental questions in the context of the terminal oxidases is the mechanism of coupling between the charge translocation processes. It is presently unclear whether these processes are directly coupled, most probably at the binuclear center, or whether instead there is an indirect coupling mediated by conformational change in the protein. Similarly, it is not known to what extent the charge transfer processes are sequential or concerted. The coupling of the electron transfer and proton transfer indicated in Figure 1 for the O→E and E→R

* Corresponding author e-mail: tjm@spawn.scs.uiuc.edu.

10.1021/jp992559v CCC: $19.00
Published on Web 12/23/1999

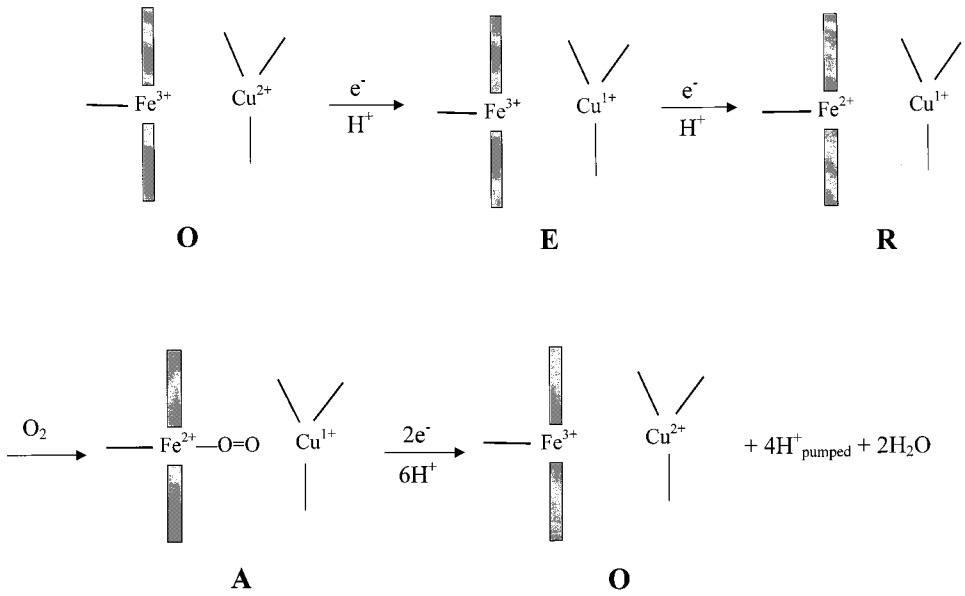

Figure 1. Schematic of the catalytic cycle in CcO. Histidine residues are denoted by lines and the porphyrin macrocycle by shaded boxes. All protons are taken up from the cytoplasm. The translocation of protons across the membrane occurs between states A and O. Metal ligands are not shown.

transitions (E and R correspond to one and two-electron reduced intermediates with respect to the fully oxidized O form, respectively) has been established experimentally.[32−35] The groups to which the proton is transferred are known to be in equilibrium with the cytoplasm and in close proximity to Fe_{a3}. This can be achieved through "proton wires"[36] extending from the binuclear center. Two channels for proton entry which could support such wires have been identified[8−10,37] and their effect on activity characterized through mutagenesis.[38] However the identity of the proton acceptor in the E and R states has not yet been identified, nor is it known whether the protons are destined to be used chemically in oxygen reduction or translocated ("pumped") across the membrane. The protonated groups could easily include either protein residues and/or hydroxide ions.

Even though the charge translocation coupling forms the driving force for interest in the terminal oxidases, many other puzzles exist whose ultimate relevance to the coupling mechanism is not known. For example, the binuclear center in the oxidized form of the enzyme is often found to be EPR-silent,[39] suggesting strong magnetic coupling[40−42] between its Cu^{2+} and Fe^{3+} ions. Thus, it was somewhat surprising to find that these ions are separated by ≈5 Å in the first X-ray crystal structures, without any indication of bridging ligands.[8,10,43] More recent structures[9,11] agree on the ion separation, but also find some electron density between the ion centers. In one structure this density was left unassigned,[9] while in the other[11] it was attributed to a peroxide ion. Furthermore, there is some degree of heterogeneity in the oxidized enzyme, with at least two distinct and reversibly interconvertible forms being possible.[44−46] These are often referred to as "fast" and "slow," indicating their propensity for reaction with CN^-. The fast form reacts ≈300 times faster than the slow form although the rate of reaction in both cases is slow compared to other oxidation states of the enzyme. Additionally, the EPR spectra of these two forms differ,[47,48] suggesting that the magnetic coupling at the binuclear center has changed. The molecular nature of these fast and slow conformers of the oxidized enzyme remains to be established and may provide important clues in the quest for a global mechanism.

The present work addresses the early steps in the CcO cycle, prior to the binding of the O_2 molecule (the O→E→R phase of the reaction cycle in Figure 1.) We have determined the energetically preferred spin states and ligands at the binuclear center, requiring an extensive search over many possible geometries, ligand combinations, and metal spin states. The theoretically predicted equilibrium structures of the binuclear center that we obtain suggest explanations for many of the ancillary puzzles described above. In accord with an electroneutrality principle,[49] both of the first two reductions are predicted to be directly coupled to protonation events in the binuclear center.

Methods

Complete quantum chemical modeling of an entire protein the size of CcO is impractical with present-day computational facilities, and is unlikely to be necessary or even desired. However, a realistic depiction of enzyme chemistry does require consideration of more than a handful of atoms. Thus, we have represented the binuclear center of CcO by a truncated fragment containing 74 atoms, depicted in Figure 2. The coordinates of all heavy atoms are taken from the bacterial X-ray structure,[10] and hydrogen atoms have been placed in minimum-energy positions using the CHARMm empirical force field.[50] The heme a_3 moiety and histidine ligands are replaced by Fe-porphine and imidazole, respectively. These substitutions represent a balance between faithful treatment of the electronic structure and computational practicality, and we comment on possible concerns below.

Given the large positive charge on the metal ions in the oxidized form of the enzyme, electroneutrality considerations lead one to expect an ionized residue in the vicinity of the binuclear center. One possible candidate is Tyr280 (residue numbering from *P. denitrificans* is used throughout this paper), lying at the end of one of the proton channels ("K-channel") leading to the binuclear center. Mutaganesis studies have shown that this residue is crucial to enzyme function,[3] and the most recent X-ray data shows it to be covalently linked to one of the histidine ligands of Cu_B.[9] Consequently, several previous workers have suggested that despite its high solution pK_a (≈10) this residue may be ionized,[11,13,38,51] and a search for its spectroscopic signature is underway.[52] The dominant effects

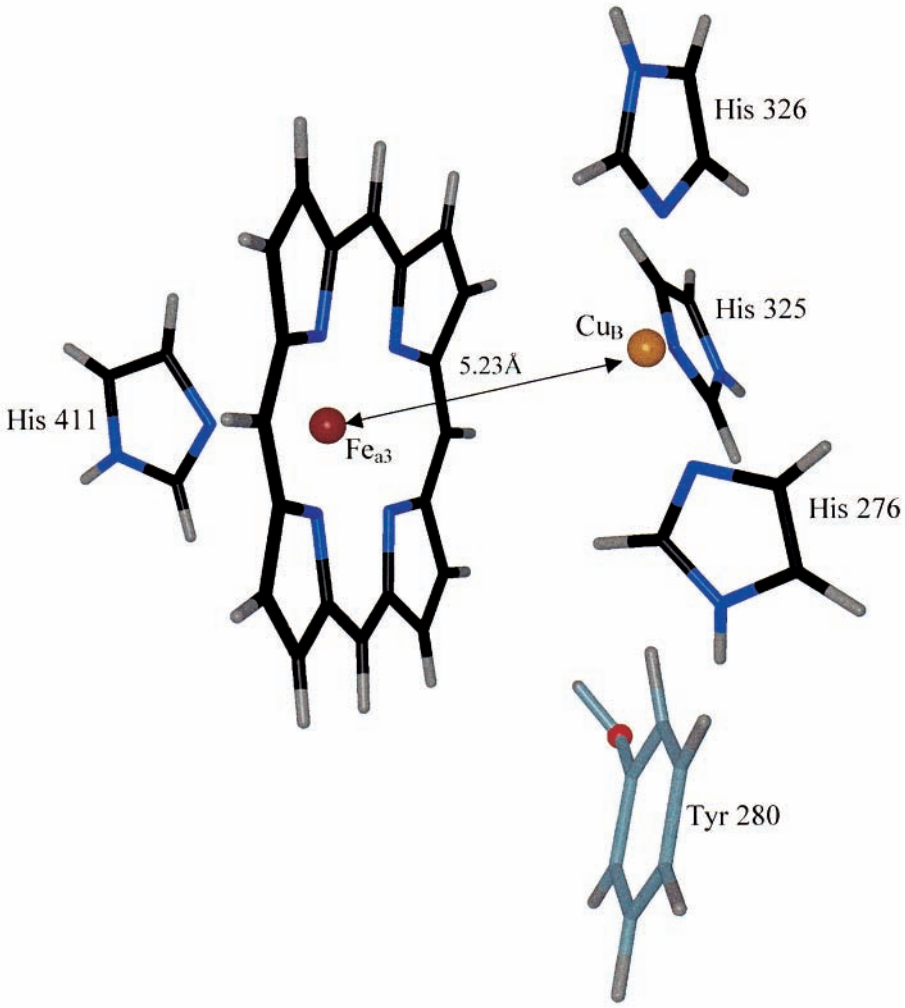

Figure 2. Computational model of the binuclear center of CcO. Carbon atoms are black, nitrogen are blue, and hydrogens are light gray. Amino acid residue numbers follow the scheme adopted for CcO from *P. denitrificans*. Heme a_3 has been replaced by Fe-porphine, and imidazole is used to represent the histidine residues. The tyrosine residue (cyan) is modeled by a unit negative point charge at the phenolic oxygen (red) when deprotonated and neglected otherwise. The model explicitly accounts for 320 electrons using 490 basis functions.

from the protonation state of Tyr280 will be electrostatic, which we include through a unit negative point charge placed at the location of the deprotonated phenolic oxygen atom. Calculations have been performed with and without this point charge, representing the deprotonated and protonated states of the Tyr280 residue, respectively.

Although the substitutions made in our model are chemically reasonable, a few caveats should be made. First, our model does not include the formyl group of heme a_3. This would affect the predicted spectroscopy of heme a_3 because this group breaks the degeneracy of the frontier molecular orbitals in the porphyrin. As we do not discuss the electronic spectra of heme a_3, this substitution is unlikely to alter the conclusions of this paper. Second, recent work[53−55] has suggested that the heme propionates may change protonation state during the reaction cycle. Our model does not admit this possibility, which could be important. We leave the refinement of the model to include the heme propionates for future work. Finally, the point charge representation of deprotonated Tyr280 ignores any electronic effect that might arise from the covalent bond linking His 276 and Tyr280. As an important part of this paper is assessing the likelihood of ionized Tyr280 in the enzymatic cycle, we have studied this last point in detail.[56] We find that the presence or absence of the covalent bond has only a minor (<2 kcal/mol) effect on the proton affinity of Tyr280.

All calculations described in this paper used an *ab initio* quantum chemical treatment, which is crucial for a faithful description of multiple oxidation and spin states of transition metal ions. The pseudospectral method[57−60] as implemented in Jaguar 3.5[61] has been used, without which computational constraints would have made the present work impractical. The restricted Hartree−Fock method is used with double-ζ basis sets[62] for all atoms and effective core potentials[63] for the transition metal ions (LAV3P basis set in Jaguar 3.5). The binuclear center is surrounded by vacuum in the calculations.

We optimized the position of OH^- and H_2O ligands for all metal spin states of the O, E, and R oxidation states of the binuclear center model described above. To prevent artifacts due to electrostatic collapse, the ligand positions have been optimized without the presence of the point charge representing Tyr280, regardless of its protonation state. Reported energetics for the ionized Tyr280 are obtained by relaxing the electronic wave function at the given nuclear configuration in the presence of the point charge. For the O state, we included up to two ligands in the active site and mixed ligands, i.e., OH^-/H_2O, were allowed. These optimizations found that structures with more than one ligand were disfavored, so at most one ligand was allowed in subsequent calculations of the E and R oxidation states. Ligands other than OH^- and H_2O are certainly possible. However, space limitations in the binuclear center make their

TABLE 1: Reaction Energies Used to Assess Relative Stability of Various Ligands in the CcO Active Site[a]

reaction	ΔE/kcal mol^{-1}
$2H_2O_{bulk} \rightarrow H_3O^+_{bulk} + OH^-_{gas}$	−170.6
$H_2O_{bulk} \rightarrow H_2O_{gas}$	−13.3
$TyrH_{gas} + H_2O_{bulk} \rightarrow Tyr^-_{gas} + H_3O^+_{bulk}$	−105.2

[a] Bulk species are modeled by immersion in a dielectric continuum ($\epsilon = 80$).

presence unlikely during turnover in active forms of the enzyme. The positions of nonligand atoms are not optimized. This is partly justified by the recent X-ray crystal structures of the O and R states which do not show major changes in the structure of the binuclear center on reduction.[11] Nevertheless, the error incurred by this assumption will increase with increasing reduction. Thus, conclusions regarding the O→E transition, in particular redox potentials, are expected to be more reliable than those for the E→R transition.

Relative energies of the optimized structures are computed assuming that H_2O is removed from bulk water in the cell (modeled as a dielectric continuum with $\epsilon = 80$) which does not interact with the binuclear center. The OH^- ligand is removed from a pair of solvated water molecules leaving solvated hydronium. The assumption that bulk solvated water molecules and ions do not interact with the binuclear center is expected to be quite good: the active site is roughly in the middle of an ≈50 Å thick membrane. The resulting reaction energies are given in Table 1.

Results

Figure 3 summarizes the relative stabilities of the final optimized geometries for the three relevant oxidation states. For clarity, only the lowest lying ligand/spin-state configurations (within 40 kcal/mol of the lowest minimum energy configuration for each oxidation state) are reported. In all cases with a single ligand, we find the ligand to be associated with Cu_B. When there are two ligands, one is associated with Cu_B and the other is not a well-defined ligand of either metal ion, as judged by the metal−ligand distance. This is shown in Table 2, where the metal−ligand distances and relative energies for all of the low-lying structures are reported. In all cases the $Fe_{a3}-O_{ligand}$ distance is greater than 2.5 Å. This is not too surprising since the Fe_{a3} is 0.7 Å out-of-plane in the *P. denitrificans* structure.

The most favorable configuration for the O state has a single OH^- ligand on Cu_B and Tyr280 is deprotonated. The active site is high spin ($S = 3$) in this configuration, corresponding nominally to ferromagnetic coupling of Fe^{3+}($S = 5/2$) and Cu^{2+}-($S = 1/2$). However, Mulliken analysis (Table 3) of the wave function reveals a surprise: the OH^- ligand is actually a hydroxyl radical, having largely donated its excess electron to the Fe_{a3} ion, which is found to be high spin ($S = 2$). Thus, the OH^- ion may be considered to be geometrically ligated to Cu_B and electronically ligated to Fe_{a3}. Certainly, this description is not expected to dominate the wave function when electron correlation and/or diffuse basis functions are included. However, it is somewhat unexpected even at the Hartree−Fock level, suggesting that the corresponding charge transfer resonance structure may have nonnegligible weight in the correlated wave function. This would provide a qualitative explanation of the observed magnetic coupling between the metal ions, as we now discuss.

The H atom of the OH^- ligand of the Cu^{2+} ion in the predicted equilibrium structure of the oxidized enzyme is directed toward the Fe^{3+} ion. Hence, this ligand is well suited

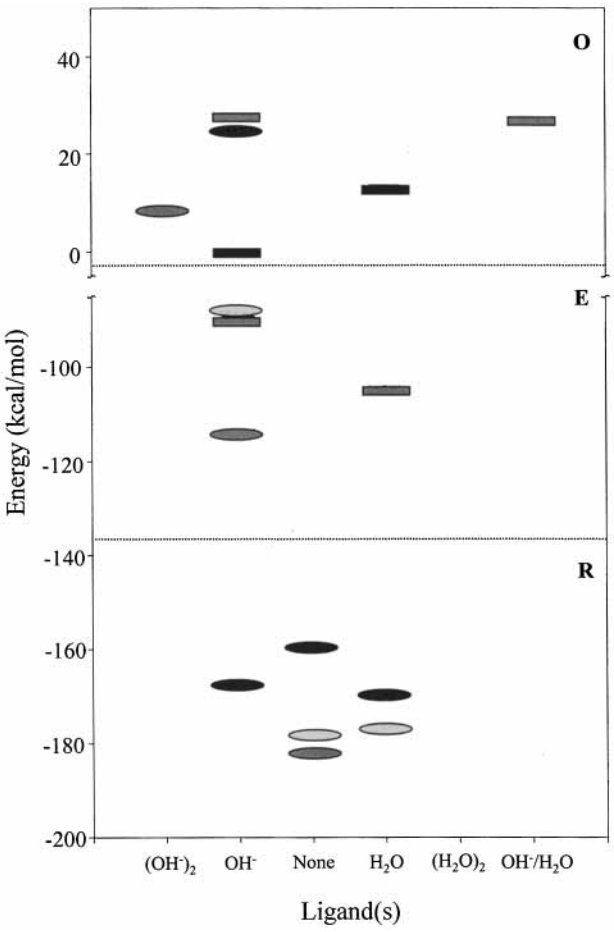

Figure 3. Relative energies of optimized configurations for the O, E, and R oxidation states of the CcO active site. For each oxidation state, only configurations which lie within 40 kcal/mol of the preferred configuration are shown. The Tyr280 residue is deprotonated/protonated for levels depicted with rectangles/ovals. Dark, medium, and light shading denotes high, intermediate, or low spin states, respectively. In all cases involving a single ligand, the ligand is associated with Cu_B. When more than one ligand is involved, the OH^- is ligated to Cu_B and the second ligand is not strongly associated with either of the metals (see Table 2).

TABLE 2: Metal−Ligand Distances (Å) and Relative Energies (kcal/mol) for the Low-Energy Configurations of the CcO Active Site in the O, E, and R Oxidation States

species	S	R_{Cu-O}		R_{Fe-O}		energy
fully oxidized (**O**)						
$Tyr^-/Cu^{2+}-H_2O/Fe^{3+}$	3	2.07		3.84		13.14
$Tyr^-/Cu^{2+}-OH^-/Fe^{3+}$-$H_2O$	2	1.97	2.72	4.69	2.87	26.46
$Tyr^-/Cu^{2+}-OH^-/Fe^{3+}$	3	2.09		3.18		0.00
$TyrH/Cu^{2+}-OH^-/Fe^{3+}$-$OH^-$	2	1.91	3.83	4.06	4.78	8.46
partially reduced (**E**)						
$TyrH/Cu^{2+}-OH^-/Fe^{2+}$	3/2	1.88		4.20		−113.74
$Tyr^-/Cu^{2+}-H_2O/Fe^{2+}$	3/2	2.04		3.27		−104.62
reduced (**R**)						
$TyrH/Cu^{1+}/Fe^{2+}$	2					−159.30
$TyrH/Cu^{1+}/Fe^{2+}$	1					−181.86
$TyrH/Cu^{1+}/Fe^{2+}$	0					−178.00
$TyrH/Cu^{1+}-H_2O/Fe^{2+}$	2	2.04		3.57		−169.55
$TyrH/Cu^{1+}-H_2O/Fe^{2+}$	0	2.16		3.56		−176.46
$TyrH/Cu^{1+}-OH^-/Fe^{2+}$	2	2.04		3.31		−167.28

to serve as the bridge which magnetically couples the metal ions, rendering the binuclear center EPR-silent. To provide a rough estimate of the magnetic coupling (J in the Heisenberg spin model) between the two ions, we have employed a minimal CI wave function to represent the intermediate ($S = 2$) spin state. This CI wave function allows only for spin recoupling

TABLE 3: Mulliken Analysis of the Electronic Wavefunctions for Low-Energy Configurations of the CcO Active Site in the O, E, and R Oxidation States[a]

species	S	Fe−Por−His	$Cu(His)_3$	Cu ligand	Fe ligand
fully oxidized (**O**)					
$Tyr^-/Cu^{2+}-H_2O/Fe^{3+}$	3	1.02	1.89	0.09	
$Tyr^-/Cu^{2+}-OH^-/Fe^{3+}-H_2O$	2	0.95	1.69	−0.67	0.03
$Tyr^-/Cu^{2+}-OH^-/Fe^{3+}$	3	0.06	1.88	0.06	
$TyrH/Cu^{2+}-OH^-/Fe^{3+}-OH^-$	2	0.00	1.68	−0.65	−0.03
partially reduced (**E**)					
$TyrH/Cu^{2+}-OH^-/Fe^{2+}$	3/2	0.00	1.65	−0.65	
$Tyr^-/Cu^{2+}-H_2O/Fe^{2+}$	3/2	0.04	1.86	0.10	
reduced (**R**)					
$TyrH/Cu^{1+}/Fe^{2+}$	2	−0.942	1.942		
$TyrH/Cu^{1+}/Fe^{2+}$	1	0.026	0.974		
$TyrH/Cu^{1+}/Fe^{2+}$	0	0.026	0.974		
$TyrH/Cu^{1+}-H_2O/Fe^{2+}$	2	−0.94	1.84	0.10	
$TyrH/Cu^{1+}-H_2O/Fe^{2+}$	0	0.00	0.92	0.07	
$TyrH/Cu^{1+}-OH^-/Fe^{2+}$	2	−0.07	0.72	−0.65	

[a] Charges are summed over all protein ligands. Thus, the $Cu(His)_3$ population includes the Cu_B ion and its three histadine (His276, His325, and His326) ligands and the Fe−Por−His population includes heme a_3 and His411.

among the six singly occupied orbitals and does not allow for orbital occupancy changes. The orbitals from the high-spin Hartree−Fock wave function are not reoptimized. From the energy difference between the S = 3 Hartree−Fock wave function and this S = 2 CI wave function, we compute J to be 1512 cm^{-1}, compared to < 1 cm^{-1} in the nonbridged oxidized binuclear center. The coupling is predicted to be ferromagnetic, as should be expected from the neglect of super-exchange effects[64] and optimal intraatomic exchange coupling.[65] Determination of the theoretical prediction for the sign and precise magnitude of the coupling constant must await further studies beyond the Hartree−Fock approximation. However, the important result is that, despite the large Fe−Cu separation, significant magnetic coupling between the two metal ions exists in the predicted ground state structure. Such coupling is indisputably observed through EPR and magnetic susceptibility experiments,[40−42,48,66] and any acceptable model must be consistent with this observation. Although the reigning experimental interpretation has been in terms of strong antiferromagnetic coupling, this has been recently questioned,[67] and the experiments can also be modeled with ferromagnetic coupling.[41]

The second lowest lying state has two OH^- ligands, with Tyr280 protonated. From Table 2, one of these is clearly ligated to Cu_B and the other is not directly ligated to either metal. It is experimentally observed that conversion from the "slow" to "fast" forms of the oxidized enzyme is achieved by raising the pH.[46] Additionally, the "slow" form exhibits an unusual g = 12 EPR signal which is not present in the "fast" form. Notice that the overall spin state of the active site is changed in this $Cu^{2+}-OH^-/Fe^{3+}-OH^-$ oxidized form: an intermediate S = 2 spin state with Fe^{3+}(S = 3/2) and Cu^{2+}(S = 1/2) is preferred over the high spin state (S = 3) expected for distant Fe^{3+}(S = 5/2) and Cu^{2+}(S = 1/2) ions. The change in the total spin for the binuclear center implies that the magnetic coupling between the metal ions is significantly perturbed in this state relative to the ground state of the oxidized enzyme. We identify this state with the "fast" form of the enzyme. Consistent with the experimental observation that the "fast" form predominates at high pH, the predicted "fast" form has an extra OH^- ligand relative to the predicted "slow" form. In accord with the EPR evidence, the magnetic coupling of the metal ions exhibits qualitative differences in the two forms. Finally, resonance Raman and magnetization experiments have suggested that Fe^{3+} is in an intermediate spin state (S = 3/2) in the "fast" form of the enzyme,[44,66] in agreement with our prediction that the overall spin of the binuclear center in this state is S = 2. In their magnetization experiments, Day and co-workers[66] found a change in sign of the zero-field splitting parameter accompanying the transition between fast and slow forms of the oxidized enzyme. They attributed this to a change in the axial ligation of Fe^{3+}, which is consistent with our suggestion that the fast form has an extra OH^- ion in the binuclear center. Direct calculation of the EPR spectrum would provide more conclusive evidence on these points.

The lowest-lying minimum for the E oxidation state has a OH^- ligand attached to Cu_B and Tyr280 is protonated. Thus, the reduction of O to E is accompanied by proton uptake at the ionized Tyr280 residue. This direct coupling of ET and PT at the binuclear center is supported by experiment,[32−35] but we are able to augment experiment with a prediction of which ligand/residue accepts the proton: the Tyr280 residue which is deprotonated in the O state. The spin state of the Fe ion is found to be intermediate, at variance with EPR experiments.[39] Since the spin state of the Fe ion in heme has been found to be very sensitive to its distance from the porphyrin plane,[68,69] this discrepancy probably comes from the fixed geometry of the nonligand atoms in our model.

Using the experimental value of 4.43 V for the absolute redox potential of the standard hydrogen electrode,[70] the computed redox potential for O → E is 507 mV. From the Mulliken analysis, this is seen to correspond to reduction of Fe_{a3}, and can thus be compared to the experimental heme a_3 redox potentials ranging[71,72] from 340 to 350 mV. Since previous attempts[73] to compute redox potentials for biological systems have often been in error by more than 1000 mV and the present results neglect entropic and zero-point energy corrections, this agreement is quite impressive and lends support to the correctness of our model. However, we note a point of disagreement: the available experimental evidence has been previously interpreted[1] to argue that the Cu^{2+} ion is reduced before the Fe^{3+} ion, as depicted in Figure 1. Further calculations are required to determine whether the agreement obtained is a consequence of cancellation of errors.

For the R oxidation state, we find three low-lying minima within 4 kcal/mol. Two of these are free of nonprotein ligands and differ only in spin state (S = 0 and S = 1). The third, which is the least favored energetically, has a single H_2O ligand associated with Cu_B. Experiments find that O_2 does not bind to the active site until it has been doubly reduced.[74] We attribute this to steric effects: there is not enough room in the active site for O_2 and a OH^- ligand, as can be surmised from the fact that few configurations with two ligands are favorable for the

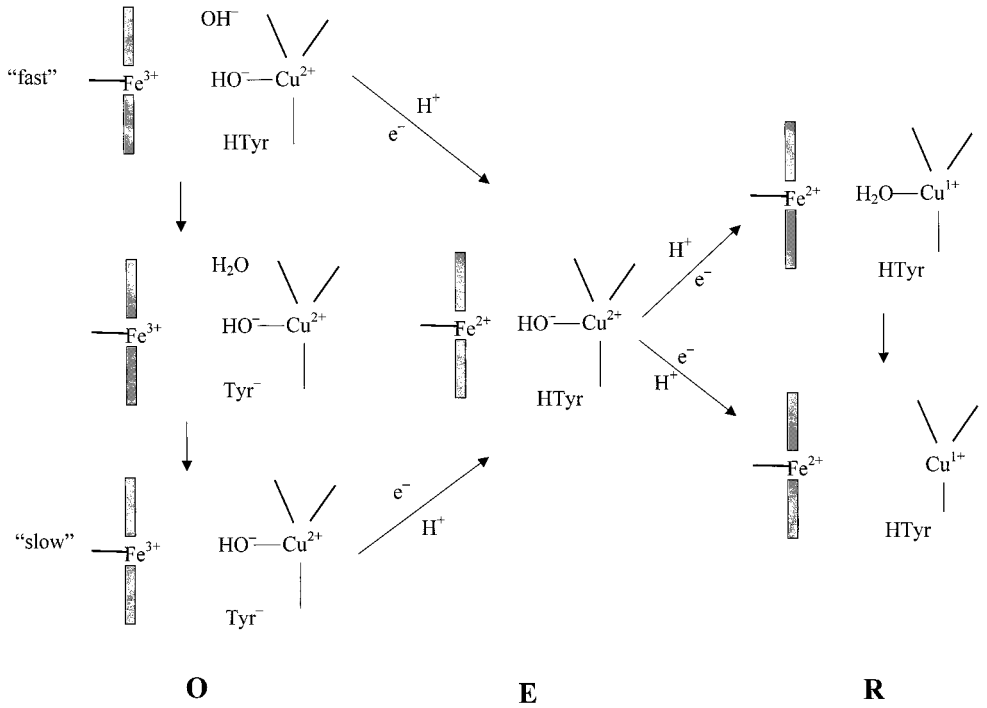

Figure 4. Proposed mechanism for the reductive half of the CcO enzyme cycle. Diagrams follow Figure 1. The two distinct conformers of the oxidized (O) enzyme are depicted along with a possible mechanism for interconversion. The two depicted structures of the reduced (R) enzyme are close in energy. Thus, what is experimentally denoted the R intermediate is likely a mixture of these.

O state. Thus, it is crucial that a low-lying configuration of the R state be free of nonprotein ligands. From the present work, we cannot determine if the H_2O ligand of Cu leaves before or during the binding of O_2. However, the H_2O ligand may play a kinetic role in directing dioxygen to Fe_{a3}. The accuracy of the redox potential for the E → R transition is expected to be quite poor because of the neglect of geometric relaxation of the proteinaceous metal ligands, and indeed we find it to be in error by more than 1000 mV.

Discussion

The present work can only be considered as a first step toward detailed understanding of the mechanism of CcO. Although we have used a large model of the active site, it completely neglects environmental effects due to the surrounding protein. The possible influence on redox potentials of protonation states for residues not included in the model must be investigated. In particular, the Glu278 residue which has been implicated as a possible switch in the pumping mechanism[12,75,76] should be considered, as well as the heme propionates.[53−55] Future work will need to include these groups and account for the electrostatic influence of the remainder of the protein. Electron correlation effects which are likely to be very important to the question of metal spin states should be included, and we have already begun work to remedy this defect of the current model. Another important point is that the work reported here does not cover the proton pumping steps of the enzymatic cycle, which also encompass the oxygen chemistry. Modeling the actual pumping will require both quantum chemistry and molecular dynamics, and the influence of the protein environment will become critical.

Even though much work remains to be done, we are able to draw some important conclusions from the current model. These are summarized in Figure 4, which presents a detailed mechanism for the reductive half of the CcO enzymatic cycle. The fully oxidized enzyme (O) is predicted to exist in two states, differing by the number of OH^- ligands. Since the O state is reached after reduction of O_2, there should be two OH^- ligands in the active site at some intermediate preceding it in the enzyme cycle. Protonation of the OH^- ligand of Fe_{a3} by Tyr280 leads to the "slow" form. On the other hand, if the OH^- ligand of Fe_{a3} "slips" off the metal ion without being protonated by Tyr280, the "fast" form is obtained. Conversion from the "fast" form to the "slow" form requires protonation of the OH^- ligand by Tyr280. Because the optimal geometry of the "fast" form has the OH^- ion located farther from the Tyr280 than it would be as a ligand of Fe_{a3}, there may be a nonnegligible barrier to this interconversion. Our results show that there is no low-lying minimum with both OH^- and H_2O ligands in the active site of the O state, so the depicted intermediate connecting the two forms can probably not be isolated. Upon one-electron reduction and protonation of the active site, the E state is reached. From the "fast" form of O, the one-electron reduction is coupled to protonation of the OH^- ligand between the metals and from the "slow" form it is coupled to reprotonation of the Tyr280 residue. Our calculations do not include dynamics and thus we cannot say which of the electron transfer and proton transfer events occur first or if it is instead a concerted process. Subsequent one-electron reduction, again coupled to proton transfer, leads to the R state. Our calculations predict a local minimum with H_2O bound to the Cu_B ion to be nearly degenerate with an active site devoid of ligands. Thus, we expect that both of the structures shown are present in the R state. Our results do not permit any statement as to whether the H_2O ligand leaves the active site before or during O_2 binding.

Conclusions

We have investigated the chemical identity and structure of metal ligands in the active site of CcO using ab initio quantum chemistry, concentrating on the first half of the enzymatic cycle, prior to oxygen binding. Our results lend support to the hypothesis that the protonation state of Tyr280 is variable during

the enzymatic reaction. Possible molecular structures for the fast and slow forms of the oxidized enzyme were identified, differing in the identity of the metal ligands. The present work is a stepping stone to more accurate models, and improvements in the treatment described here are currently underway.

Acknowledgment. We thank Profs. R. B. Gennis and K. Schulten for useful discussions. We are also grateful to an unknown referee for detailed comments and suggestions. This work was supported by Research Corporation (RI-0085) and the National Institutes of Health (P41 RR05969). T.J.M. is grateful to the NSF and Research Corporation for CAREER and Research Innovation Awards, respectively. D.B.M. thanks the Hovorka Foundation and the University of Illinois for graduate fellowships. Figure 2 was created with VMD[77] and Raster3D.[78] The programs CHARMm and QUANTA have been developed by Molecular Simulations, Inc.

References and Notes

(1) Malatesta, F.; Antonini, G.; Sarti, P.; Brunori, M. *Biophys. Chem.* **1995**, *54*, 1.

(2) Solomon, E. I.; Sundaram, U. M.; Machonkin, T. E. *Chem. Rev.* **1996**, *96*, 2563.

(3) Trumpower, B. L.; Gennis, R. B. *Annu. Rev. Biochem.* **1994**, *63*, 675.

(4) Ferguson-Miller, S.; Babcock, G. T. *Chem. Rev.* **1996**, *96*, 2889.

(5) Anson, F. C.; Shi, C.; Steiger, B. *Acc. Chem. Res.* **1997**, *30*, 437.

(6) Collman, J. P.; Schwenninger, R.; Rapta, M.; Broring, M.; Fu, L. *Chem. Comm.* **1999**, *2*, 137.

(7) Collman, J. P.; Rapta, M.; Broring, M.; Raptova, L.; Schwenninger, R.; Boitrel, B.; Fu, L.; L'Her, M. *J. Am. Chem. Soc.* **1999**, *121*, 1387.

(8) Tsukihara, T.; Aoyama, H.; Yamashita, E.; Tomizaki, T.; Yamaguchi, H.; Shinzawa-Itoh, K.; Nakashima, R.; Yaono, R.; Yoshikawa, S. *Science* **1995**, *269*, 1069.

(9) Ostermeier, C.; Harrenga, A.; Ermler, U.; Michel, H. *Proc. Natl. Acad. Sci. U.S.A.* **1997**, *94*, 10547.

(10) Iwata, S.; Ostermeier, C.; Ludwig, B.; Michel, H. *Nature* **1995**, *376*, 660.

(11) Yoshikawa, S.; Shinzawaitoh, K.; Nakashima, R.; Yaono, R.; Yamashita, E.; Inoue, N.; Yao, M.; Fei, M. J.; Libeu, C. P.; Mizushima, T.; Yamaguchi, H.; Tomizaki, T.; Tsukihara, T. *Science* **1998**, *280*, 1723.

(12) Hofacker, I.; Schulten, K. *Proteins* **1998**, *30*, 100.

(13) Kannt, A.; Roy, C.; Lancaster, D.; Michel, H. *Biophys. J.* **1998**, *74*, 708.

(14) Goddard, W. A., III.; Olafson, B. D. *Proc. Natl. Acad. Sci. U.S.A.* **1975**, *72*, 2335−2339.

(15) Bair, R. A.; Goddard, W. A., III. *J. Am. Chem. Soc.* **1977**, *99*, 3505−3507.

(16) Olafson, B. D.; Goddard, W. A., III. *Proc. Natl. Acad. Sci. U.S.A.* **1977**, *74*, 1315−1319.

(17) Bair, R. A.; Goddard, W. A., III. *J. Am. Chem. Soc.* **1978**, *100*, 5669−5676.

(18) Takeuchi, T.; Gray, H. B.; Goddard, W. A., III. *J. Am. Chem. Soc.* **1994**, *116*, 9730.

(19) Brameld, K.; Dasgupta, S.; Goddard, W. A., III. *J. Phys. Chem. B* **1997**, *101*, 4851−4859.

(20) Brameld, K. A.; Shrader, W. D.; Imperiali, B.; Goddard, W. A., III. *J. Mol. Biol.* **1998**, *280*, 913−923.

(21) Brameld, K. A.; Goddard, W. A., III. *J. Am. Chem. Soc.* **1999**, *121*, 985−993.

(22) Avdeev, V. I.; Upton, T. H.; Weinberg, W. H.; Goddard, W. A., III. *Surf. Sci.* **1980**, *95*, 391−402.

(23) Steigerwald, M. L.; Goddard, W. A., III. *J. Am. Chem. Soc.* **1985**, *107*, 5027−35.

(24) Carter, E. A.; Goddard, W. A., III. *Organometallics* **1988**, *7*, 675−686.

(25) Carter, E. A.; Goddard, W. A., III. *Surf. Sci.* **1989**, *209*, 243−289.

(26) Irikura, K. K.; Goddard, W. A., III. *J. Am. Chem. Soc.* **1994**, *116*, 8733−8740.

(27) Perry, J. K.; Ohanessian, G.; Goddard, W. A., III. *Organometallics* **1994**, *13*, 1870−1877.

(28) Bierwagen, E. P.; Bercaw, J. E.; Goddard, W. A., III. *J. Am. Chem. Soc.* **1994**, *116*, 1481−1489.

(29) Siegbahn, P. E. M.; Crabtree, R. H. *J. Am. Chem. Soc.* **1999**, *121*, 117.

(30) Pavlov, M.; Seigbahn, P. E. M.; Blomberg, M. R. A.; Crabtree, R. H. *J. Am. Chem. Soc.* **1998**, *120*, 548.

(31) Yoshioka, Y.; Kubo, S.; Yamaguchi, K.; Saito, I. *Chem. Phys. Lett.* **1998**, *294*, 459.

(32) Capitanio, N.; Vygodina, T. V.; Capitanio, G.; Konstantinov, A. A.; Nicholls, P.; Papa, S. *Biochim. Biophys. Acta* **1997**, *1318*, 255.

(33) Mitchell, R.; Rich, P. R. *Biochim. Biophys. Acta* **1994**, *1186*, 19.

(34) Hallen, S.; Brzezinski, P.; Malmström, B. G. *Biochemistry* **1994**, *33*, 1467.

(35) Ädelroth, P.; Sigurdson, H.; Hallen, S.; Brzezinski, P. *Proc. Natl. Acad. Sci. U.S.A.* **1996**, *93*, 12292.

(36) Nagle, J. F.; Morowitz, H. J. *Proc. Natl. Acad. Sci. U.S.A.* **1978**, *75*, 298.

(37) Riistama, S.; Hummer, G.; Puustinen, A.; Dyer, R. B.; Woodruff, W. H.; Wikström, M. *FEBS Lett.* **1997**, *414*, 275.

(38) Gennis, R. B. *Biochim. Biophys. Acta* **1998**, *1365*, 241.

(39) Van Gelder, B. F.; Beinert, H. *Biochim. Biophys. Acta* **1969**, *189*, 1.

(40) Barnes, Z. K.; Babcock, G. T.; Dye, J. L. *Biochemistry* **1991**, *30*, 7597.

(41) Tweedle, M. F.; Wilson, L. J.; Garcia-Iniguez, L.; Babcock, G. T.; Palmer, G. *J. Biol. Chem.* **1978**, *253*, 8065.

(42) Moss, T. H.; Shapiro, E.; King, T. E.; Beinert, H.; Hartzell, C. *J. Biol. Chem.* **1978**, *253*, 8072.

(43) Yoshikawa, S.; Shinzawa-Itoh, K.; Tsukihara, T. *J. Bioenerg. Biomembr.* **1998**, *30*, 7.

(44) Carter, K. R.; Antalis, T. M.; Palmer, G.; Ferris, N. S.; Woodruff, W. H. *Proc. Natl. Acad. Sci. U.S.A.* **1981**, *78*, 1652.

(45) Watmough, N. J.; Cheesman, M. R.; Gennis, R. B.; Greenwood, C.; Thomson, A. J. *FEBS Lett.* **1993**, *319*, 151.

(46) Palmer, G. *J. Bioenerg. Biomembr.* **1993**, *25*, 145.

(47) Baker, G. M.; Noguchi, M.; Palmer, G. *J. Biol. Chem.* **1987**, *262*, 595.

(48) Brudvig, G. W.; Morse, R. H.; Chan, S. I. *J. Magn. Reson.* **1986**, *67*, 189.

(49) Rich, P. R. *Ann. J. Plant. Physiol.* **1995**, *22*, 479.

(50) MacKerell, A. D.; Bashford, D.; Bellott, M.; Dunbrack, R. L.; Evanseck, J. D.; Field, M. J.; Fischer, S.; Gao, J.; Ha, S.; Joseph-McCarthy, D.; Kuchnir, L.; Kuczera, K.; Lau, F. T. K.; Mattos, C.; Michnick, S.; Ngo, T.; Nguyen, D. T.; Prodhom, B.; Reiher, W. E.; Roux, B.; Schlenkrich, M.; Smith, J. C.; Stote, R.; Straub, J.; Watanabe, M.; Wiorkiewicz-Kuczera, J.; Yin, D.; Karplus, M. *J. Phys. Chem.* **1998**, *102B*, 3586.

(51) Rottenberg, H. *Biochim. Biophys. Acta* **1998**, *1364*, 1.

(52) Gennis, R. B., private communication.

(53) Behr, J.; Hellwig, P.; Mantele, W.; Michel, H. *Biochemistry* **1998**, *37*, 7400.

(54) Rost, B.; Behr, J.; Hellwig, P.; Richter, O. M. H.; Ludwig, B.; Michel, H.; Mantele, W. *Biochemistry* **1999**, *38*, 7565.

(55) Michel, H. *Proc. Natl. Acad. Sci. U.S.A.* **1998**, *95*, 12819.

(56) Moore, D. B.; Martínez, T. J., in preparation.

(57) Friesner, R. A. *Chem. Phys. Lett.* **1985**, *116*, 39.

(58) Friesner, R. A. *Annu. Rev. Phys. Chem.* **1991**, *42*, 341.

(59) Langlois, J. M.; Muller, R. P.; Coley, T. R.; Goddard, W. A., III.; Ringnalda, M. N.; Won, Y.; Friesner, R. A. *J. Chem. Phys.* **1990**, *92*, 7488−7497.

(60) Martínez, T. J.; Carter, E. A. Pseudospectral Methods Applied to the Electron Correlation Problem. In *Modern Electronic Structure Theory, Part II*; Yarkony, D., Ed.; World Scientific Press: Singapore, 1995; p 1132.

(61) Jaguar v3.5; Schrodinger, Inc.: Portland, OR, 1998.

(62) Hehre, W. J.; Ditchfield, R.; Pople, J. A. *J. Chem. Phys.* **1972**, *56*, 2257.

(63) Hay, P. J.; Wadt, W. R. *J. Chem. Phys.* **1985**, *82*, 270.

(64) Anderson, P. W. Exchange in Insulators: Superexchange, Direct Exchange, and Double Exchange. In *Magnetism*; Rado, G. T., Ed.; Academic Press: New York, 1963; Vol. 1; p 25.

(65) Voter, A. F.; Goodgame, M. M.; Goddard, W. A., III. *Chem. Phys.* **1985**, *98*, 7−14.

(66) Day, E. P.; Peterson, J.; Sendova, M. S.; Schoonover, J.; Palmer, G. *Biochemistry* **1993**, *32*, 7855.

(67) Oganesyan, V. S.; Butler, C. S.; Watmough, N. J.; Greenwood, C.; Thomson, A. J.; Cheesman, M. R. *J. Am. Chem. Soc.* **1998**, *120*, 4232.

(68) Rovira, C.; Kunc, K.; Hutter, J.; Ballone, P.; Parrinello, M. *J. Phys. Chem.* **1997**, *101A*, 8914.

(69) Rovira, C.; Carloni, P.; Parrinello, M. *J. Phys. Chem.* **1999**, *103B*, 7031.

(70) Reiss, H.; Heller, A. *J. Phys. Chem.* **1985**, *89*, 4207−4213.

(71) Carithers, R. P.; Palmer, G. *J. Biol. Chem.* **1981**, *256*, 7967.

(72) Schroedl, N.; Hartzell, C. R. *Biochemistry* **1977**, *16*, 4961.

(73) Fisher, C. L.; Chen, J.-L.; Li, J.; Bashford, D.; Noodleman, L. *J. Phys. Chem.* **1996**, *100*, 13498.

(74) Chance, B.; Saronio, C.; Leigh, J. S. *J. Biol. Chem.* **1975**, *250*, 9226.
(75) Verkhovskaya, M. L.; Garcia-Horsman, A.; Puustinen, A.; Rigaud, J.-L.; Morgan, J. E.; Verkhovsky, M. I.; Wikström, M. *Proc. Natl. Acad. Sci. U.S.A.* **1997**, *94*, 10128.
(76) Hummer, G.; Garcia, A. E.; Soumpasis, D. M. *Biophys. J.* **1995**, *68*, 1639.
(77) Humphrey, W. F.; Dalke, A.; Schulten, K. *J. Mol. Graphics* **1996**, *14*, 33.
(78) Merritt; Bacon. *Methods Enzymol.* **1997**, *277*, 505.